

Article

Free Energy Analyses of Cell-Penetrating Peptides Using the Weighted Ensemble Method

Seungho Choe ^{1,2} 

- ¹ Department of Energy Science & Engineering, Daegu Gyeongbuk Institute of Science & Technology (DGIST), Daegu 42988, Korea; schoe@dgist.ac.kr
² Energy Science & Engineering Research Center, Daegu Gyeongbuk Institute of Science & Technology (DGIST), Daegu 42988, Korea

Abstract: Cell-penetrating peptides (CPPs) have been widely used for drug-delivery agents; however, it has not been fully understood how they translocate across cell membranes. The Weighted Ensemble (WE) method, one of the most powerful and flexible path sampling techniques, can be helpful to reveal translocation paths and free energy barriers along those paths. Within the WE approach we show how Arg₉ (nona-arginine) and Tat interact with a DOPC/DOPG(4:1) model membrane, and we present free energy (or potential mean of forces, PMFs) profiles of penetration, although a translocation across the membrane has not been observed in the current simulations. Two different compositions of lipid molecules were also tried and compared. Our approach can be applied to any CPPs interacting with various model membranes, and it will provide useful information regarding the transport mechanisms of CPPs.

Keywords: cell-penetrating peptides; free energy; weighted ensemble method; electrostatics



Citation: Choe, S. Free Energy Analyses of Cell-Penetrating Peptides Using the Weighted Ensemble Method. *Membranes* **2021**, *11*, 974. <https://doi.org/10.3390/membranes11120974>

Academic Editor: Natalia Wilke

Received: 31 October 2021
Accepted: 1 December 2021
Published: 9 December 2021

Publisher's Note: MDPI stays neutral with regard to jurisdictional claims in published maps and institutional affiliations.



Copyright: © 2021 by the author. Licensee MDPI, Basel, Switzerland. This article is an open access article distributed under the terms and conditions of the Creative Commons Attribution (CC BY) license (<https://creativecommons.org/licenses/by/4.0/>).

1. Introduction

Cell-penetrating peptides (CPPs) have been extensively studied for a long time since they are capable of transporting various cargoes (e.g., proteins, peptides, DNAs, and even small drugs) into cells [1]. Various factors, including the concentration of CPPs and the properties of the membrane affect the transport mechanisms of CPPs [2,3]. It has been known that the translocation mechanisms of different families of CPPs are not the same, and most CPPs can have more than a single pathway depending on the experimental conditions such as a concentration of CPPs [4].

Arginine (R)-rich peptides have been extensively studied because of their effectiveness in translocation [2,5]. One of the possible scenarios for the insertion of R-rich peptides into the lipid bilayer is a strong interaction with negatively charged phospholipid heads.

Molecular dynamics (MD) simulations have been used to investigate functional properties of various CPPs and their interactions with many different lipids; however, the mechanism of translocation of CPPs and interactions with lipids are still under debate.

Herce et al. [6,7] showed in their MD simulations that the attractive interactions between the Arg₉ (or Tat) peptides and the phosphate groups of the phospholipids results in significant local distortions of the bilayer, and these distortions lead to the formation of a toroidal pore. However, Herce et al.'s simulation was criticized by Yesylevskyy et al. [8] that the spontaneous translocation of CPPs in MD simulations is not expected within a short time scale (100~200 ns). It is believed that the time required for the translocation of CPP is on the order of minutes [9].

It is unclear that we can observe the translocation of CPPs across the membranes using conventional all-atom MD simulations. However, an MD simulation is still one of valuable tools to study protein-lipid interactions, and it can provide us with detailed information such as the contribution of electrostatic energy between CPPs and the membranes, effects of water molecules, etc. In our previous work [10], we found that the electrostatic interaction

between Arg₉ and a DOPC/DOPG(4:1) membrane plays a role at the initial stage of translocation. We also quantitatively showed that several water molecules coordinated by Arg₉ increased during the penetration, and this led to a membrane thinning and a decreased bending rigidity of the membrane. However, we could not find a translocation of Arg₉ across the membrane within a 1 μ s time scale.

Due to the short time scale achieved in current MD simulations, people have been using biased simulations (e.g., umbrella sampling [11–13], steered MD simulations [14]) to study CPPs and their interactions with membranes. The umbrella sampling is very popular to obtain free energy barrier between CPPs and membranes. However, people have noticed that there could be an artifact in the free energy analysis due to a short simulation time in each window.

In this study, we implement a weighted ensemble (WE) method [15] in our MD simulations (see more in the Section 2). The WE method is one of very flexible path sampling techniques and it is easy to implement. A detailed review was given by Zuckerman and Chong [15]. We use the WESTPA software [16,17], which has been widely applied to various systems, ranging from atomistic to cellular scale. It turns out that the WE method is very effective for studying interactions between CPPs and membranes and for obtaining free energy barriers in the current study.

First, we apply the WE method to Arg₉ with a DOPC/DOPG(4:1) membrane used in the previous study [10] as well as Tat with identical lipids. Only a few simulations used mixtures of lipids (e.g., a mixture of DOPC/DOPG or DOPC/DOPE) so far, and it is still unclear whether the surface charge of a membrane affects the translocation of CPPs. For example, a DOPC/DOPG(1:1) membrane appeared the better host for the translocation of KR9C in experiments [18] and the fluorescence probe carboxyfluorescein-labeled R9 (CF-R9) translocates continuously across the lipid membrane of single DOPG/DOPC(2/8), DOPG/DOPC(4/6), and DLPG/DTPC(2/8) giant unilamellar vesicles (GUVs) and enters these GUVs without pore formation [19]. However, Hecce et al. showed in their experiments that DOPG lipids are not necessary for the Arg₉ peptides to penetrate bilayers [7]. Thus, we also simulate two different lipid compositions, DOPC/DOPE(4:1) and DOPC lipids, respectively, to see if the surface charge of model membranes affects the penetration of CPPs. Then, the free energy barriers between CPPs and model membranes can be obtained using the WE simulation data, and these free energy calculations will be helpful to understand the transport mechanisms of CPPs.

2. Methods

2.1. Equilibrium Simulations

All simulations were performed using the NAMD package [20] and CHARMM36 force field [21]. The following systems were well equilibrated before starting the WE simulations: 4 Arg₉ with a DOPC/DOPG(4:1) membrane (System I), 4 Tat with a DOPC/DOPG(4:1) membrane (System II), 4 Arg₉ with a DOPC/DOPE(4:1) membrane (System III), and 4 Arg₉ with a DOPC membrane (System IV). CHARMM-GUI [22] was used to setup a DOPC/DOPG(4:1) membrane, a DOPC/DOPE(4:1) membrane, a DOPC membrane and TIP3P water molecules. The DOPC/DOPG(4:1) mixture consists of 76 DOPC and 19 DOPG lipids in each layer in System I. The same model membrane was used in System II. System III has a DOPC/DOPE(4:1) mixture which consists of 80 DOPC and 20 DOPE lipids in each layer. System IV has 95 DOPC lipids in each layer. K and Cl ions were added in each system to make a concentration of 150 mM. All Arg₉ (in System I, III, and IV) or Tat (in System II) peptides were initially located in the upper solution, and they were bound to the upper layer during the equilibration.

The NPT simulations were performed at T = 310K. Temperature and pressure were kept constant using Langevin dynamics. An external electric field (0.05 V/nm) was applied in the negative z-direction (from CPPs to the membrane) as suggested in previous work [7,23] and also in our previous simulations [10] to account for the transmembrane potential [24]. The particle-mesh Ewald (PME) algorithm was used to compute the elec-

tric forces, and the SHAKE algorithm was used to allow a 2 fs time step during the whole simulations.

In the case of System I, we use a pre-equilibrated structure in the previous study [10], which was equilibrated up to 1 μ s. System II was also equilibrated for at least 1 μ s. The other two systems (System III and IV) were equilibrated for 100 ns before starting the WE simulations. This time scale is enough for CPPs to close to model membranes. Figure S1 (see Supplementary Information) shows both an initial setup and a snapshot after equilibration for each system, and Figure S2 presents radial distribution functions of the followings: phosphorus atoms vs. water, phosphorus atoms vs. oxygen in water, ester oxygen vs. oxygen in water. These plots show that the quality of hydration of membranes is very similar to each other. During the equilibration, CPPs were confined in the upper water box so that there is no interaction between CPPs and the lower leaflet of model membranes. Whenever a CPP is leaving the upper water box, a small force was applied to pull that CPP inside the box. All CPPs in each system were well contacted with the lipid molecules after the equilibration, and then the WE simulations were performed using those equilibrated systems.

2.2. Weighted Ensemble (WE) Simulations

We use the WESTPA (The Weighted Ensemble Simulation Toolkit with Parallelization and Analysis) software package [16,17] to enable the simulation of rare events, for example, translocation of CPPs across a model membrane. WESTPA is an open source, and its utility has been proved for a broad range of problems. All WE trajectories are unbiased and hence used to calculate conditional probabilities or transition rates.

To use the WE method in MD simulations, we need to define a progress coordinate, several bins, several walkers (child simulations) in each bin, and a time interval for splitting and combining trajectories [17]. We define the progress coordinate as a distance in z-direction between the center of mass of phosphorus atoms in the upper leaflet and that of a CPP (Arg₉ or Tat). After equilibration of each system, an initial distance between phosphorus atoms and a CPP was measured, and boundaries were set using this initial position and the position of the center of the membrane, for example, $[-18 \text{ \AA} \text{ (the center of membrane), } 3 \text{ \AA} \text{ (the initial distance)}]$. Each bin size was 0.25 \AA and, the number of walkers in each bin was 5. The time interval for splitting and combining the trajectories was set 5 ps during all the WE simulations. The progress coordinate was calculated using MDAnalysis [25]. The potential mean of force (PMF) profiles were obtained from each WE simulation data using “w_pdist” and “plohist” codes in the WESTPA package [16,17].

3. Results

3.1. WE Simulations Show Much-Enhanced Penetration within a Short Amount of Time

We observe that both Arg₉ and Tat penetrate through the middle of the model membrane during the WE simulations; however, translocation across the membrane has not been observed in the current simulations.

Figure 1 shows the penetration depth of both Arg₉ and Tat vs. the number of iterations of each WE simulation. Here, we define the penetration depth as a distance between the center of mass of CPP and that of phosphorus atoms of the upper leaflet. The penetration depth of Arg₉ in the previous equilibrium simulation was about $-6 \sim -7 \text{ \AA}$ [10], and the current WE simulation shows -17.6 \AA and -17.7 \AA for Arg₉ and Tat, respectively. The initial positions of Arg₉ and Tat after equilibration are different from each other; however, they quickly penetrate the DOPC/DOPG(4:1) membrane. Please note that these plots show only one of the trajectories of each simulation which shows the maximum penetration depth. Multiple trajectories cannot reach the middle of the membrane. As one can see in the figure, the penetration depth changes a lot within a very short time scale. As described in the Section 2 each iteration corresponds to 5 ps and the figure shows that both CPPs reach their maximum penetration depth within a very short time scale (3~5 ns) after the

WE simulation started. Therefore, the WE method provides us with a very effective tool to overcome potential energy barriers.

Figure 2 presents snapshots of both Arg₉ and Tat, which show the maximum penetration depth during the WE simulation. The yellow shows each CPP, and gray is the lipids. The blue and red are phosphorus atoms of the upper and the lower leaflets. Water molecules, ions, and the other three CPPs are omitted for clarity. As one can see in Figure 2, the membrane is deformed a lot when Arg₉ or Tat penetrates the middle of the membrane. Figure S3 in Supplementary Information shows membrane curvature more clearly. As shown in the previous simulation [10], several water molecules around a CPP is increased when the CPP penetrates the membrane, and a membrane thinning is also observed in the current WE simulations.

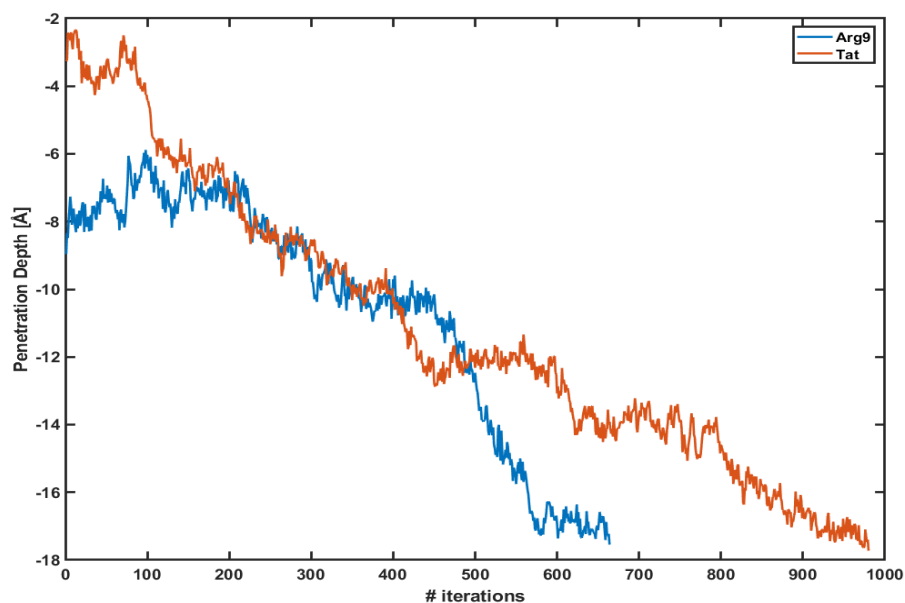


Figure 1. The penetration depth of Arg₉ (blue line) and Tat (red line) vs. several iterations.

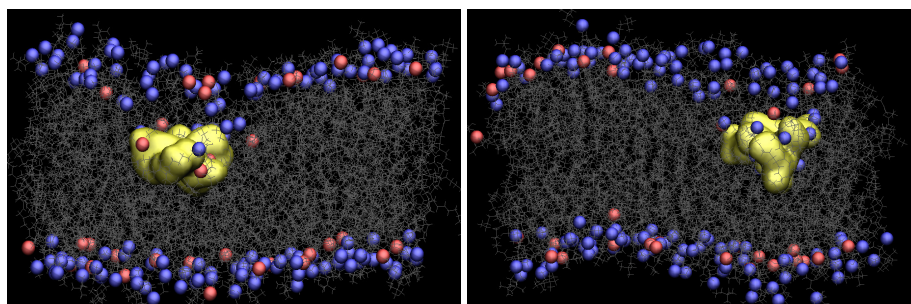


Figure 2. Snapshots of Arg₉ (left) and Tat (right) with a DOPC/DOPG(4:1) model membrane (yellow: CPP, gray: lipids, blue and red: phosphorus atoms of DOPC and DOPG, respectively).

3.2. Electrostatic Energy between a CPP and a Model Membrane Plays a Role during the Translocation

In our previous equilibrium simulation of Arg₉ with a DOPC/DOPG(4:1) membrane, we showed that electrostatic energy between Arg₉ and the membrane is strongly correlated with the penetration depth of Arg₉ [10]. This proved that electrostatic interaction between a CPP and a membrane is essential at the early translocation stage [26].

We calculate the same electrostatic energy between Arg₉ (or Tat) and the membrane. We want to see if there is still a strong correlation between electrostatic energy and penetration depth during the WE simulations. We use two trajectories in Figure 1 to calculate electrostatic energy.

Figure 3 presents the penetration depth (left axis, black line) vs. electrostatic energy (right axis, blue line) between Arg₉ and the lipid molecules within 15 Å of Arg₉. The red dotted line is an average over every 30 iterations. The figure shows that an absolute magnitude of electrostatic energy becomes smaller when Arg₉ rapidly penetrates inside the membrane (e.g., between 450th ~ 550th iterations). Therefore, one can expect that the penetration increases as the magnitude of electrostatic energy becomes smaller.

We find similar behavior in the case of Tat. Figure 4 shows the same energy calculation for Tat. The red dotted line is an average over every 30 iterations as before. The penetration increases gradually as the magnitude of electrostatic energy becomes smaller.

At the initial stage of translocation, it is well known that the interaction between positive charges of CPPs and a negative part of lipid molecules is essential for binding. The current simulations show that electrostatic interaction between CPPs and membranes still plays a role during the translocation of CPPs. In System I and System II Arg₉ and Tat strongly interact with DOPG lipids, and the translocation seems not easy. However, our simulations show that the translocation of CPPs is possible even in this strong electrostatic interaction. During the translocation, the electrostatic interaction should be diminished. We conjecture that water molecules play a role to make electrostatic energy weaker. As shown in the previous work [10], several water molecules around CPPs are increased during the translocation.

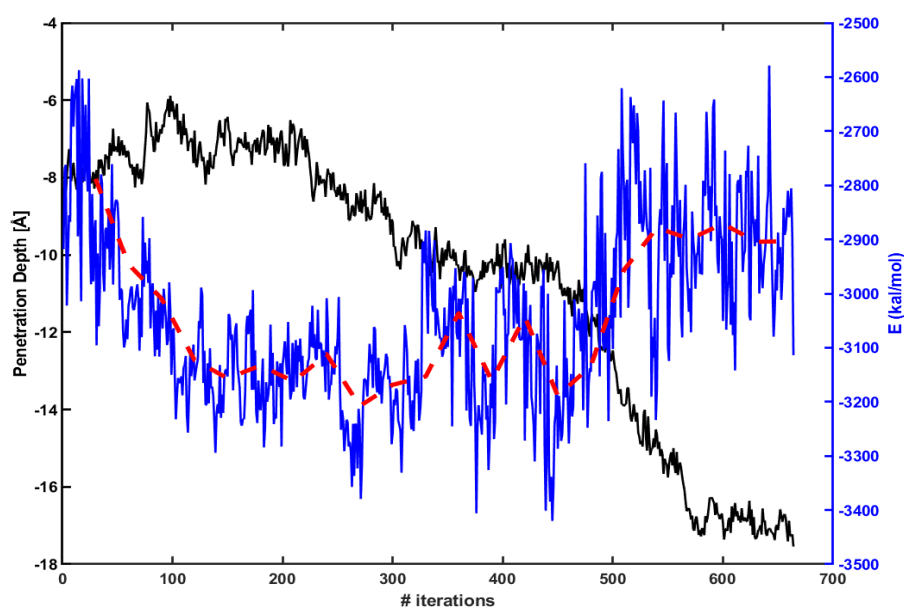


Figure 3. The penetration depth of Arg₉ (left axis, black line) vs. electrostatic energy between Arg₉ and lipids molecules within 15 Å of Arg₉ (right axis, blue line). The red dotted line is an average over every 30 iterations.

3.3. The Free Energy Profiles Based on the WE Simulation Data Show That Arg₉ Penetrates through a DOPC/DOPG(4:1) Model Membrane Much Easier Than Tat Does

This section presents the potential mean of force (PMF) profiles of Arg₉ and Tat along the penetration paths shown in Figure 1. Another advantage of using the WE method is that it provides a free energy analysis without any biased sampling (e.g., umbrella sampling) [17]. Therefore, these PMF profiles will tell us how much potential energy barriers exist along those paths and which CPP can penetrate the membrane more efficiently.

Figure 5 shows the PMF profiles of both Arg₉ and Tat as a function of a progress coordinate (or reaction coordinate). We use a penetration depth as the progress coordinate. The progress coordinate becomes negative when Arg₉ and Tat penetrate below the upper leaflet of the membrane. The blue line is the PMF profile for Arg₉ and the red line for Tat. One can notice that the free energy of Arg₉ is much lower than that of Tat. Figure 5 shows that a free energy barrier is about 100 kT for Arg₉ to reach the middle of the membrane

while it is about 280 kT for Tat to reach a similar position. This means that Arg₉ penetrates the DOPC/DOPG(4:1) membrane much easier than Tat does. However, these analyses can depend on the type of model membranes, and we cannot conclude that Arg₉ is always more efficient for penetrating membranes than Tat regardless of membrane types. The order of magnitude of free energy for Arg₉ (~100 kT) is very similar to a previous result [27], which used umbrella samplings. On the other hand, Tat's order of magnitude of free energy is much higher than those of previous simulations [8,13]. Please note that most of the previous free energy analyses were done with a single lipid molecule (e.g., DOPC or DPPC), while we use a mixed composition of lipid molecules (DOPC/DOPG(4:1)) in our simulations. Although the magnitude of free energy can depend on systems studied, the observed tendency between Arg₉ and Tat is consistent with experimental results [28,29] which showed more efficient cellular uptake of Arg₉ than Tat.

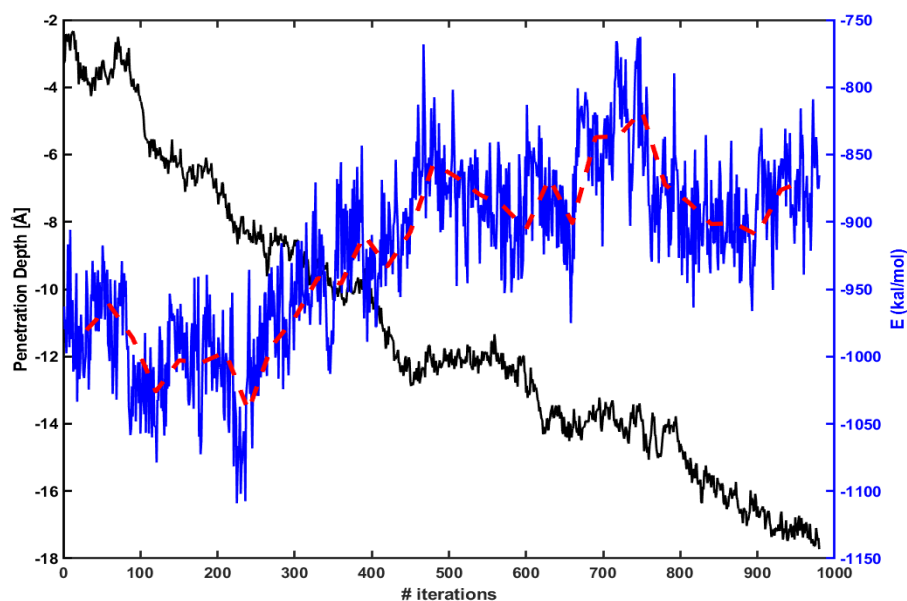


Figure 4. Same as in Figure 3 , but for Tat.

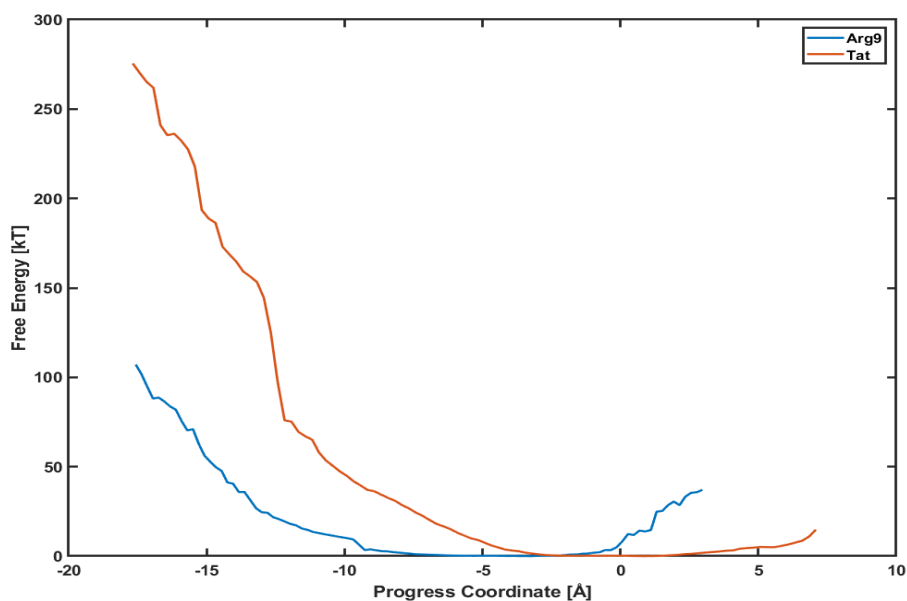


Figure 5. Comparison of potential mean of force (PMF) between Arg₉ (blue line) and Tat (red line).

3.4. Different Lipid Compositions Slightly Affect the PMF Profiles of Arg₉

It is interesting to see whether a different lipid composition can affect the penetration depth and the PMF profile. Figure 6 presents the PMF profiles of Arg₉ with DOPC/DOPG(4:1) lipids, DOPC/DOPE(4:1) lipids, and DOPC lipids, respectively. The blue line is for Arg₉ with DOPC/DOPG(4:1) lipids shown already in Figure 5. The red one is for Arg₉ with DOPC/DOPE(4:1) lipids and the orange for Arg₉ with DOPC lipids. DOPC and DOPE lipids are neutral, while DOPG lipids are negatively charged. We want to see if the translocation of CPPs strongly correlates with the lipid types, e.g., the charge of membranes.

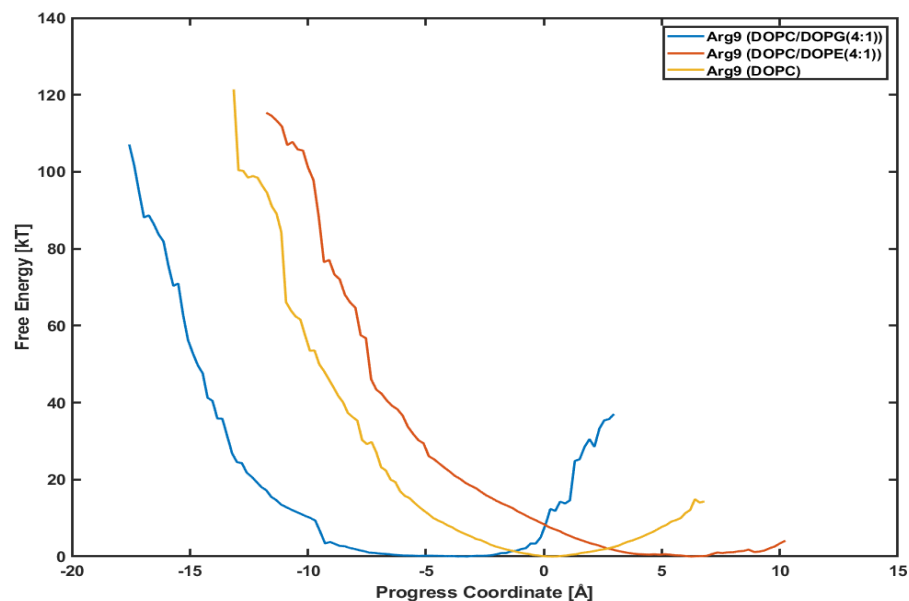


Figure 6. Comparison of potential mean of force (PMF). Arg₉ with a DOPC/DOPG(4:1) (blue line), a DOPC/DOPE(4:1) (red line), and a DOPC (orange line), respectively.

The minimum point in each plot is different from each other because the initial position of each CPP after equilibration is not the same. Although the initial positions are different from each other, the slope of each plot looks very similar to each other. Although Arg₉ in System III (with DOPC/DOPE(4:1) lipids) and Arg₉ in System IV (with DOPC lipids) have not reached the final position as of System I (with DOPC/DOPG(4:1)), the similar slope means similar variations in free energy. Based on these plots, we can conjecture that the penetration of Arg₉ is not much dependent on the lipid composition, and the effect of surface charge is minimal.

4. Discussion

Both Arg₉ and Tat do not show any translocation across the model membranes during the WE simulations. However, the WE method can be helpful to identify the transport mechanisms of CPPs and interactions between CPPs and lipid molecules because conventional equilibrium MD simulations have difficulty in sampling. Free energy (potential mean of force, PMF) profiles can be obtained without any biased simulation (e.g., umbrella sampling) within the WE approach. The WE simulation and its free energy analyses can be used to study the efficiency of penetration of CPPs.

Is it possible to observe the translocation if we simulate much longer? Currently, both Arg₉ and Tat are stuck in the hydrophobic core. They can stay in the hydrophobic core for a long time even if we simulate much longer. They can move up and down a little, but it is not likely to move in either direction, moving back or forward. A visual inspection shows that they are trapped inside the hydrophobic core. The lipids make a small cage around CPPs so that CPPs cannot move easily. It seems that a single CPP cannot cause further

deformation of the membrane at the current stage, and thus it is difficult to move. There is a possibility that the free energy barriers along the downward direction are much higher than those along the upward direction. In that case, it is easier for CPPs to go back to the hydrophilic region where they started. It will be interesting to try the WE simulations from the current positions of both Arg9 and Tat to the hydrophilic area outside, i.e., the positive z-direction. Then, we will obtain another free energy profiles for both Arg9 and Tat, and these profiles will give us a clue.

There are still some limitations in our WE simulations. First, a time scale of each trajectory shown in Figure 1 is less than 10 ns. Please note that the total simulation time for each CPP simulation is about 5~10 μ s, which includes all the walkers (child simulations) in each bin and all the iterations. This time scale of a single trajectory might be too short to observe a water pore mentioned in the previous results [8,13,27,30]. Second, our PMF profiles are incomplete because we do not find any translocation of CPPs and PMF profiles spanned only from the top to the middle of the model membranes. It has been known that free energy barriers between CPPs and membranes are changed in the presence of a water pore. For example, Huang et al. [27] reported that the free energy becomes lower in the presence of a water pore. This confirms the previous results from MD simulations and a continuum modeling which calculate the free energy of a single arginine residue for translocating across a membrane [31–34]. We need more WE simulation data points to complete the free energy profiles, which include translocation of CPP across the membranes and the effect of the water pore. Third, we have not attached any cargo to Arg9 (or Tat) in the current study. We expect that the conformational changes both in CPP and the model membranes depend on a type of cargo. CPPs are commonly used with attaching negatively charged molecules and thus the total charge of the system decreases or becomes closer to neutral. It is not clear whether the overall charge of the whole system or only the charge of CPP is essential for the internalization. Most electronic neutral CPPs are usually far less powerful than cationic or amphiphilic CPPs. However, the electronic neutral cyclic peptide cyclosporin A (CsA) can have stronger (5-fold or 19-fold) penetrating capacity than other neutral peptides and its penetrating capacity was as strong as Tat [35]. On the other hand, in the case of oligoarginine (R_n : $n = 4, 8, 12, 16$) R_{12} and R_{16} showed more efficient uptake than R_4 and R_8 [36]. If only the charge of CPP is essential during the translocation, we can compare the free energy barriers of these oligoarginine within the WE method and identify their penetration efficiency.

It has been known that it is difficult for a single CPP to make a pore and to make a translocation across the membrane [8]. One of the key factors which makes the water pore is a concentration of CPPs. In our WE simulations, the P(protein)-L(lipids) ratio was 0.042 or 0.05, and these concentrations maybe not be enough to observe the translocation across the membrane. Another critical factor for translocating CPPs is pH dependence. Experimental results showed the uptake of CPPs depends on pH values [37,38], and the uptake of CPPs is enhanced at low pH. It is worth trying MD simulations at low pH to see if any changes in conformational changes both in CPPs and in the model membranes. There has been significant progress in the development of constant pH molecular dynamics (pHMD) techniques [39,40] and this approach with the WE method would be good to reveal the pH dependence in interactions between CPPs and the model membranes.

Our simulations show characteristics of both the carpet-like model [41] and the membrane thinning model [42]. It is interesting to note that an orientation (a direction from the N-terminal to the C-terminal) of CPPs (Arg9 or Tat) in our simulations is almost parallel to the membrane, and its orientation is changed a little during the entire simulation. This could be one of the reasons that it is difficult for a single CPP to make a water pore. In this work, the progress coordinate was set for a single CPP, and it was difficult to observe aggregation of CPPs in a local area. To make a water pore, a collective behavior between CPPs seems to be essential, and a high concentration of CPPs would be needed. It is worth using an increased concentration of CPPs and implementing a progress coordinate as a distance between the center of mass of the phosphorus atoms of the upper leaflet and that

of more than a single CPP (e.g., two Arg₉ or two Tat). However, the penetration of two CPPs seems much slower than using a single CPP.

Supplementary Materials: The following are available online at <https://www.mdpi.com/article/10.3390/membranes11120974/s1>. The Supplementary Information (SI), which includes Figure S1 (initial structures), Figure S2 (radial distribution functions), and Figure S3 (membrane curvature).

Funding: This work was supported by the Faculty start-up fund from DGIST and by the DGIST R&D Program of the Ministry of Science and ICT (21-BRP-12).

Institutional Review Board Statement: Not applicable.

Informed Consent Statement: Not applicable.

Data Availability Statement: The data that support the findings of this study are available from the corresponding author upon reasonable request.

Acknowledgments: The author would like to thank the DGIST Supercomputing Big Data Center for computing resources and the National Supercomputing Center with supercomputing resources including technical support (KSC-2021-CRE-0296).

Conflicts of Interest: The author declares no conflict of interest.

Abbreviations

The following abbreviations are used in this manuscript:

CPP	Cell-Penetrating Peptide
WE	Weighted Ensemble
DNA	DeoxyriboNucleic Acid
DOPC	1,2-dioleoyl-sn-glycero-3-phosphocholine
DOPG	1,2-dioleoyl-sn-glycero-3-[phospho-rac-(1-glycerol)]
DOPE	1,2-dioleoyl-sn-glycero-3-phosphoethanolamine
Arg ₉ (R9)	a peptide with RRRRRRRRR
Tat	a peptide with GRKKRRQRRPPQ

References

- Guidotti, G.; Brambilla, L.; Rossi, D. Cell-Penetrating Peptides: From basic research to clinics. *Trends Pharmacol. Sci.* **2017**, *38*, 406–424. [[CrossRef](#)] [[PubMed](#)]
- Ruseska, I.; Zimmer, A. Internalization mechanisms of cell-penetrating peptides. *Beilstein J. Nanotechnol.* **2020**, *11*, 101–123. [[CrossRef](#)] [[PubMed](#)]
- Pisa, M.D.; Chassaing, G.; Swiecicki, J. Translocation Mechanism(s) of Cell-Penetrating Peptides: Biophysical Studies Using Artificial Membrane Bilayers. *Biochemistry* **2015**, *54*, 194–207. [[CrossRef](#)] [[PubMed](#)]
- Madani, F.; Lindberg, S.; Langel, U.; Futaki, S.; Gräslund, A. Mechanisms of cellular uptake of cell-penetrating peptides. *J. Biophys.* **2011**, *2011*, 1–10. [[CrossRef](#)]
- Fretz, M.M.; Penning, N.A.; Al-Taei, S.; Futaki, S.; Takeuchi, T.; Nakase, I.; Storm, G.; Jones, A.T. Temperature-, concentration- and cholesterol-dependent translocation of L- and D-octa-arginine across the plasma and nuclear membrane of CD34⁺ leukaemia cells. *Biochem. J.* **2007**, *403*, 335–342. [[CrossRef](#)] [[PubMed](#)]
- Herce, H.D.; Garcia, A.E. Molecular dynamics simulations suggest a mechanism for translocation of the HIV-1 TAT peptide across lipid membranes. *Proc. Natl. Acad. Sci. USA* **2007**, *104*, 20805–20810. [[CrossRef](#)]
- Herce, H.D.; Garcia, A.E.; Litt, J.; Kane, R.S.; Martin, P.; Enrique, N.; Rebolledo, A.; Milesi, V. Arginine-rich peptides destabilize the plasma membrane, consistent with a pore formation translocation mechanism of cell-penetrating peptides. *Biophys. J.* **2009**, *97*, 1917–1925. [[CrossRef](#)] [[PubMed](#)]
- Yesylevskyy, S.; Marrink, S.J.; Mark, A. Alternative mechanisms for the interaction of the cell-penetrating peptides penetratin and the TAT peptide with lipid bilayers. *Biophys. J.* **2009**, *97*, 40–49. [[CrossRef](#)]
- Zorko, M.; Langel, U. Cell-penetrating peptides: Mechanism and kinetics of cargo delivery. *Adv. Drug Deliv. Rev.* **2005**, *57*, 529–545. [[CrossRef](#)]
- Choe, S. Molecular dynamics studies of interactions between Arg₉(nona-arginine) and a DOPC/DOPG(4:1) membrane. *AIP Adv.* **2020**, *10*, 105103. [[CrossRef](#)]
- Pourmousa, M.; Wong-ekkabut, J.; Patra, M.; Karttunen, M. Molecular Dynamic Studies of Transportan Interacting with a DPPC Lipid Bilayer. *J. Phys. Chem. B* **2013**, *117*, 230–241. [[CrossRef](#)]

12. Teseia, G.; Vazdarb, M.; Jensenc, M.R.; Cragnella, C.; Masond, P.E.; Heydae, J.; Skepo, M.; Jungwirthd, P.; Lunda, M. Self-association of a highly charged arginine-rich cell-penetrating peptide. *Proc. Natl. Acad. Sci. USA* **2017**, *114*, 11428–11433. [[CrossRef](#)] [[PubMed](#)]
13. Choong, F.H.; Yap, B.K. Cell-Penetrating Peptides: Correlation between peptide-lipid interaction and penetration efficiency. *ChemPhysChem* **2021**, *22*, 493–498. [[CrossRef](#)]
14. Akhunzada, M.J.; Chandramouli, B.; Bhattacharjee, N.; Macchi, S.; Cardarelli, F.; Brancato, G. The role of Tat peptide self-aggregation in membrane pore stabilization: Insights from a computational study. *Phys. Chem. Chem. Phys.* **2017**, *19*, 27603–27610. [[CrossRef](#)] [[PubMed](#)]
15. Zuckerman, D.M.; Chong, L.T. Weighted Ensemble Simulation: Review of Methodology, Applications, and Software. *Annu. Rev. Biophys.* **2017**, *46*, 43–57. [[CrossRef](#)]
16. Bogetti, A.T.; Mostolan, B.; Dickson, A.; Pratt, A.; Saglam, A.S.; Harrison, P.O.; Adelman, J.L.; Dudek, M.; Torrillo, P.A.; DeGrave, A.J.; et al. A Suite of Tutorials for the WESTPA Rare-Events Sampling Software. *Living J. Comp. Mol. Sci.* **2019**, *1*, 10607.
17. Zwier, M.C.; Adelman, J.L.; Kaus, J.W.; Pratt, A.J.; Wong, K.F.; Rego, N.B.; Suarez, E.; Lettieri, S.; Wang, D.W.; Grabe, M.; et al. WESTPA: An interoperable, highly scalable software package for weighted ensemble simulation and analysis. *J. Chem. Theory Comput.* **2015**, *11*, 800–809. [[CrossRef](#)]
18. Crosio, M.A.; Via, M.A.; Cámara, C.I.; Mangiarotti, A.; Pópolo, M.G.D.; Wilke, N. Interaction of a polyarginine peptide with membranes of different mechanical properties. *Biomolecules* **2019**, *9*, 625–642. [[CrossRef](#)]
19. Sharmin, S.; Islam, M.Z.; Karal, M.A.S.; Shibly, S.U.A.; Dohra, H.; Yamazaki, M. Effects of Lipid Composition on the Entry of Cell-Penetrating Peptide Oligoarginine into Single Vesicles. *Biochemistry* **2016**, *55*, 4154–4165. [[CrossRef](#)]
20. Phillips, J.; Braun, R.; Wang, W.; Gumbart, J.; Tajkhorshid, E.; Villa, E.; Chipot, C.; Skeel, R.D.; Kale, L.; Schulten, K. Scalable molecular dynamics with NAMD. *J. Comput. Chem.* **2005**, *26*, 1781–1802. [[CrossRef](#)]
21. Brooks, B.R.; Brooks, C.L., III; Mackerell, A.D., Jr.; Nilsson, L.; Petrella, R.J.; Roux, B.; Won, Y.; Archontis, G.; Bartels, C.; Boresch, S.; et al. CHARMM: The biomolecular simulation program. *J. Comput. Chem.* **2009**, *30*, 1545–1614. [[CrossRef](#)]
22. Jo, S.; Kim, T.; Iyer, V.G.; Im, W. CHARMM-GUI: A web-based graphical user interface for CHARMM. *J. Comput. Chem.* **2008**, *29*, 1859–1865. [[CrossRef](#)] [[PubMed](#)]
23. Walrant, A.; Vogel, A.; Correia, I.; Lequin, O.; Olausson, B.E.S.; Desbat, B.; Sagan, S.; Alves, I.D. Membrane interactions of two arginine-rich peptides with different cell internalization capacities. *Biochim. Biophys. Acta* **2012**, *1818*, 1755–1763. [[CrossRef](#)] [[PubMed](#)]
24. Roux, B. The membrane potential and its representation by a constant electric field in computer simulations. *Biophys. J.* **2008**, *95*, 4205–4216. [[CrossRef](#)] [[PubMed](#)]
25. Michaud-Agrawal, N.; Denning, E.J.; Woolf, T.B.; Beckstein, O. MDAAnalysis: A Toolkit for the Analysis of Molecular Dynamics Simulations. *J. Comput. Chem.* **2011**, *32*, 2319–2327. [[CrossRef](#)]
26. Galassi, V.; Wilke, N. On the Coupling between Mechanical Properties and Electrostatics in Biological Membranes. *Membranes* **2021**, *11*, 478. [[CrossRef](#)]
27. Huang, K.; Garcia, A.E. Free energy of translocating an arginine-rich cell-penetrating peptide across a lipid bilayer suggests pore formation. *Biophys. J.* **2013**, *104*, 412–420. [[CrossRef](#)]
28. Qian, Z.; Martyna, A.; Hard, R.L.; Wang, J.; Appiah-Kubi, G.; Coss, C.; Phelps, M.A.; Rossman, J.S.; Pei, D. Discovery and Mechanism of Highly Efficient Cyclic Cell-Penetrating Peptides. *Biochemistry* **2016**, *55*, 2601–2612. [[CrossRef](#)]
29. Guterstam, P.; Madani, F.; Hirose, H.; Takeuchi, T.; Futaki, S.; Andaloussi, S.E.; Gräslund, A.; Langel, Ü. Elucidating cell-penetrating peptide mechanisms of action for membrane interaction, cellular uptake, and translocation utilizing the hydrophobic counter-anion pyrenebutyrate. *Biochim. Biophys. Acta* **2009**, *1788*, 2509–2517. [[CrossRef](#)]
30. Islam, M.Z.; Sharmin, S.; Moniruzzaman, M.; Yamazaki, M. Elementary processes for the entry of cell-penetrating peptides into lipid bilayer vesicles and bacterial cells. *Appl. Microbiol. Biotech.* **2018**, *102*, 3879–3892. [[CrossRef](#)]
31. Freitas, J.A.; Tobias, D.J.; von Heijne, G.; White, S.H. Interface connections of a transmembrane voltage sensor. *Proc. Natl. Acad. Sci. USA* **2005**, *102*, 15059–15064. [[CrossRef](#)]
32. Dorairaj, S.; Allen, T.W. On the thermodynamic stability of a charged arginine side chain in a transmembrane helix. *Proc. Natl. Acad. Sci. USA* **2007**, *104*, 4943–4948. [[CrossRef](#)]
33. MacCallum, J.L.; Bennett, W.F.D.; Tieleman, D.P. Partitioning of amino acid side chains into lipid bilayers: Results from computer simulations and comparison to experiment. *J. Gen. Physiol.* **2007**, *129*, 371–377. [[CrossRef](#)] [[PubMed](#)]
34. Choe, S.; Hecht, K.A.; Grabe, M. A continuum method for determining protein insertion energies and the problem of charged residues. *J. Gen. Physiol.* **2008**, *131*, 563–573. [[CrossRef](#)] [[PubMed](#)]
35. Gao, W.; Yang, X.; Lin, Z.; He, B.; Mei, D.; Wang, D.; Zhang, H.; Zhang, H.; Dai, W.; Wang, X.; et al. The use of electronic-neutral penetrating peptides cyclosporin A to deliver pro-apoptotic peptide: A possibly better choice than positively charged TAT. *J. Control. Release* **2017**, *261*, 174–186. [[CrossRef](#)] [[PubMed](#)]
36. Kosuge, M.; Takeuchi, T.; Nakase, I.; Jones, A.T.; Futaki, S. Cellular Internalization and Distribution of Arginine-Rich Peptides as a Function of Extracellular Peptide Concentration, Serum, and Plasma Membrane Associated Proteoglycans. *Bioconjugate Chem.* **2008**, *19*, 656–664. [[CrossRef](#)]
37. Sun, C.; Shen, W.C.; Tu, J.; Zaro, J.L. Interaction between Cell-Penetrating Peptides and Acid-Sensitive Anionic Oligopeptides as a Model for the Design of Targeted Drug Carriers. *Mol. Pharm.* **2014**, *11*, 1583–1590. [[CrossRef](#)] [[PubMed](#)]

38. Ouahab, A.; Cheraga, N.; Onoja, V.; Shen, Y.; Tu, J. Novel pH-sensitive charge-reversal cell penetrating peptide conjugated PEG-PLA micelles for docetaxel delivery: In vitro study. *Int. J. Pharm.* **2014**, *466*, 233–245. [[CrossRef](#)]
39. Chen, W.; Morrow, B.H.; Shi, C.; Shen, J.K. Recent development and application of constant pH molecular dynamics. *Mol. Simul.* **2014**, *40*, 830–838. [[CrossRef](#)] [[PubMed](#)]
40. Radak, B.K.; Chipot, C.; Suh, D.; Jo, S.; Jiang, W.; Phillips, J.C.; Schulten, K.; Roux, B. Constant-pH Molecular Dynamics Simulations for Large Biomolecular Systems. *J. Chem. Theory Comput.* **2017**, *13*, 5933–5944. [[CrossRef](#)]
41. Pouny, Y.; Rapaport, D.; Mor, A.; Nicolas, P.; Shai, Y. Interaction of antimicrobial dermaseptin and its fluorescently labeled analogues with phospholipid membranes. *Biochemistry* **1992**, *31*, 12416–12423. [[CrossRef](#)] [[PubMed](#)]
42. Lee, M.T.; Hung, W.C.; Chen, F.Y.; Huang, H.W. Manybody effect of antimicrobial peptides: On the correlation between lipid's spontaneous curvature and pore formation. *Biophys. J.* **2005**, *89*, 4006–4016. [[CrossRef](#)] [[PubMed](#)]